

RSC Advances



This is an *Accepted Manuscript*, which has been through the Royal Society of Chemistry peer review process and has been accepted for publication.

Accepted Manuscripts are published online shortly after acceptance, before technical editing, formatting and proof reading. Using this free service, authors can make their results available to the community, in citable form, before we publish the edited article. This *Accepted Manuscript* will be replaced by the edited, formatted and paginated article as soon as this is available.

You can find more information about *Accepted Manuscripts* in the [Information for Authors](#).

Please note that technical editing may introduce minor changes to the text and/or graphics, which may alter content. The journal's standard [Terms & Conditions](#) and the [Ethical guidelines](#) still apply. In no event shall the Royal Society of Chemistry be held responsible for any errors or omissions in this *Accepted Manuscript* or any consequences arising from the use of any information it contains.



Journal Name

COMMUNICATION

Lipid membrane formation on chemical gradient modified surfaces

Received 00th January 20xx,
Accepted 00th January 20xx

Ying Zhang, Xuejing Wang, Shenghua Ma, Kunpeng Jiang, Xiaojun Han*

DOI: 10.1039/x0xx00000x

www.rsc.org/

The relationship between surface wetting property and lipid membrane status formed via giant unilamellar vesicle rupture were investigated using chemical gradient surfaces. Fluorescence microscopy and AFM analysis confirmed that GUVs could form uniform monolayer, monolayer patches and bilayer patches on surface regions with contact angle range from 108° to ~61°, ~60° to ~55° and less than 5°, respectively. The intact GUVs stand in the area with contact angle between ~54° and ~28°.

Supported lipid membranes, including monolayers and bilayers, serve as excellent model system for studying the properties of cell membrane, such as mobility and phase separation process, as well as provide a natural environment for protein immobilization.^{1,2} One of the classical approaches for preparation of supported lipid membranes is vesicle fusion method. This process of lipid membranes formation is highly sensitive to the surface wetting property. It is well known that the amphipathic structure of phospholipids lead to the formation of bilayer on hydrophilic surface³ and monolayer on hydrophobic substrate⁴. However the specific range of surface contact angle for the formation of both types of lipid membranes is still not clear. However, the study of this relationship is challenging because there is loads of work for the preparation of almost a hundred of substrates with various contact angles. The sample to sample variation is also very difficult to avoid.

The gradient surfaces, including chemical gradients and topography gradients, have been demonstrated to be a powerful system in many studies in the chemical, physical, and biological science.⁵⁻⁷ A number of methods have been used to prepare surface gradients. Luk et al. fabricated a gold film with gradient nanotopography using varying angle vapor deposition to investigate the adhesion of mammalian cells.⁸ Xu et al. prepared mussel-inspired polydopamine (PDA) gradients on

different surfaces by simply immersing substrates into a dopamine solution at a tilt angle.⁹ Moreover, some gradient surfaces could generate a contact angle gradient simultaneously. Among them, the space limited plasma oxidization method could create the substrate with both chemical gradient and contact angle gradient.¹⁰

Giant unilamellar vesicles (GUVs) were rarely used to study the process of vesicle fusion method.¹¹⁻¹³ Most relevant reports were based on the small unilamellar vesicles (SUVs) rather than GUVs (larger than 1 μm in diameter)¹⁴. However, because the size of GUVs is closer to that of mammalian cells, they play a more crucial role in studying the dynamics and structural features of cells, including budding and endocytosis,¹⁵⁻¹⁷ etc.

Herein we investigated the influence of surface with different contact angle on supported lipid membrane formation using GUVs, and found out 4 regions with various types of lipid membranes, which may provide clues for the surface wetting property influence on cell immobilization.

In order to form the contact angle gradient substrates, the exposure time in air plasma should be decided firstly. To this aim, the power of the plasma was fixed at 80 W and the exposure time of TODS SAMs modified substrates in air plasma was varied from 10 s to 160 s. From Fig. S1 it is noted that the contact angle decreases from 108° to ~5° as the exposure time increases to 120 s, and levelled off afterwards. Therefore 2 min was chosen as the exposure time.

A freshly prepared SAM modified substrate covered by a silicon wafer with an extremely thin spacer at one end to form a "wedge" shape space, as show in Fig. 1a, was loaded in the plasma generator for 2 min to create the chemical gradient surface. The contact angle of the resultant surface was measured from position 1 to 3 along the middle line (dash line shown in Fig. 1a) as shown in Fig. 1c. It is clear to see that a gradient surface has been created by this way. The initially hydrophobic surface (108°) became gradually hydrophilic from position of 0 mm to 5 mm (position 1 to 2 in Fig. 1a). The depth of the gradient is about 80°. In the area between 5 mm to 7 mm (position 2 to 3 in Fig. 1a), the contact angles are

State Key Laboratory of Urban Water Resource and Environment, School of Chemical Engineering and Technology, Harbin Institute of Technology, 92 West Da-Zhi Street, Harbin, 150001, China. Email: hanxiaojun@hit.edu.cn

† Electronic Supplementary Information available: [details of any supplementary information available should be included here]. See DOI: 10.1039/x0xx00000x

constant. The images of water droplets in different position, shown in Fig. 1c, also confirmed the formation of gradient surface. The relationship between the contact angle range (region c1-c4 in Fig. 1c) and lipid membrane formation will be illustrated in the following section.

The gradient substrates were incubated in GUVs solution for 2 h, followed by rinsing with abundant water to remove the residual GUVs. Fig. 2a shows the fluorescence microscopy images of the finally substrates along the dash line in Fig. 1a. The perpendicular dark lines in this image are unreal, which are caused by the dim marginal area of the fluorescence microscope. Getting rid of this problem, when we linked the image with the contact angle of the substrate shown in Fig. 1c, it could be found that the substrate can be divided into four parts, including homogeneous area (on the strongly hydrophobic surface with contact angle from 108° - 61° , Fig. a1), patches (on the weakly hydrophobic surface, $\sim 60^\circ$ - $\sim 55^\circ$, Fig. a2), bright spots (on the surface with contact angle between 54° and 28° , Fig. a3) and bright patches (on the surface contact angle less than 5° Fig. a4). In order to get more detailed information, higher resolution microscopy images of different areas were taken (Fig. 2b). From these close-up pictures, it can be observed clearly that the bright spots in Figure a3 are GUVs attached on the surface (Fig. 2b3). The features of GUVs observed here are in consistent with those of free GUVs (Fig. S2), which leads us to propose the membrane states in region c3 are intact GUVs. There is homogenous membrane

and bright patches on area of a1 and a4 respectively, because the area a1 is very hydrophobic surface and area a4 is hydrophilic surface. The lipid membranes on them should be lipid monolayer and lipid bilayer respectively. Moreover, according to the fluorescence intensity analysis, under same experiment condition the value of fluorescence intensity in Fig. b1 and b2 is 50% of that in Fig. b4, because there are only as half number of lipid in the monolayer as that in the bilayer on the same size of area. Meanwhile, the average size of patches in Fig. 2b2 is $36.12 \pm 1.8 \mu\text{m}^2$, which is properly as twice big as that in the Fig. b4 ($19.7 \pm 2.4 \mu\text{m}^2$). This result also confirms that they are monolayer and bilayer respectively, because the size of monolayer is equal to the size of inner leaflet plus that of the outer leaflet of GUVs. The formations of lipid membranes in different regions were schematically depicted at the bottom row of Fig. b.

To further characterize the lipid membranes, AFM images and section profiles were obtained (Fig. 2c). Height of defects in Fig. c1 and lipid membrane patch in Fig. c2 is 2.45 nm and 2.62 nm respectively, which confirms the lipid membrane formed on the contact angle range of 108° - $\sim 55^\circ$ is lipid monolayer. Whereas the height of lipid membrane prepared on contact angle less than 5° is 5.15 nm, which proves the membrane in this area is lipid bilayer. The height analysis is in accordance with the results of fluorescence microscopy images in this study.

Therefore, it can be concluded that lipid monolayer was formed on the surface with strongly hydrophobic property ($\sim 61^\circ$ - $\sim 108^\circ$); the monolayer patches were formed on the weakly hydrophobic surface ($\sim 55^\circ$ - $\sim 60^\circ$); GUVs were intactly attached on the surface with contact angle from $\sim 28^\circ$ to $\sim 54^\circ$; lipid bilayer patches were formed on the hydrophilic area where the contact angle is less than 5° . It is noteworthy that, the minimum lipid concentration for preparation of uniform monolayer on the surface with contact angle range from $\sim 61^\circ$ - $\sim 108^\circ$ is $1 \mu\text{g mL}^{-1}$.

The physical mechanism behind the formation uniform monolayers with GUVs fusion on hydrophobic surface locally relates the surface energy between the hydrophobic SAM surface and the vesicle solution. The high energy aroused by the exposure of a hydrophobic surface to an aqueous environment is thermodynamically unfavourable, which leads to vesicle rupture and fusion spontaneously to form lipid monolayer on top of SAM surface.¹² As for the lipid bilayer formation process, the high curvature caused by the deformation of GUV strongly adsorbed on the hydrophilic surface plays a critical role.¹¹ Obviously, the rupture of GUVs could dissipate the energetically unstable situation provided by the highly curved region. On the other hand, in the medium range of contact angle region ($\sim 28^\circ$ - $\sim 54^\circ$), vesicles "stood" on the substrate because the surface energy is not sufficient enough to drive vesicles to rupture. As for the region with partially plasma oxidation ($\sim 55^\circ$ - $\sim 60^\circ$), polar functional groups, including carboxyl, aldehyde and hydroxyl group, could promote H-bond formation between water molecules and substrate interface, consequently to reduce the surface free

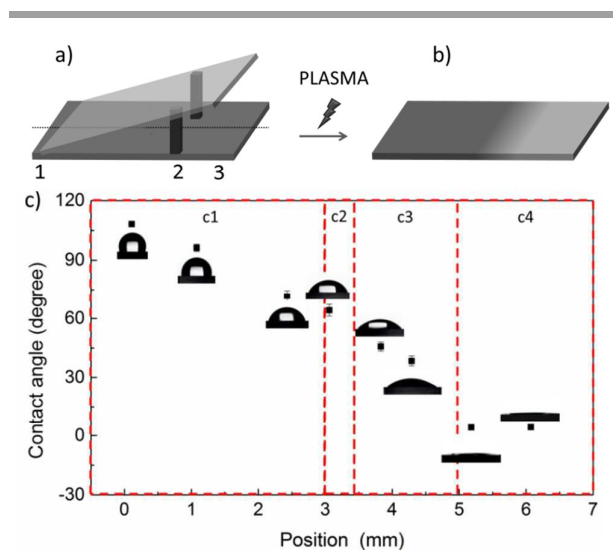


Fig. 1 The schematic of SAMs gradient fabrication using space limited plasma oxidation technique (not to scale) and the contact angle data along the gradient. a) The sample block including a SAM modified bottom substrate. (b) The grayscale gradient from left to right on the sample represents chemical gradient after plasma oxidation. c) The contact angle data and water droplet images (side view) as a function of distance starting from position 1 to 3 in 1a.

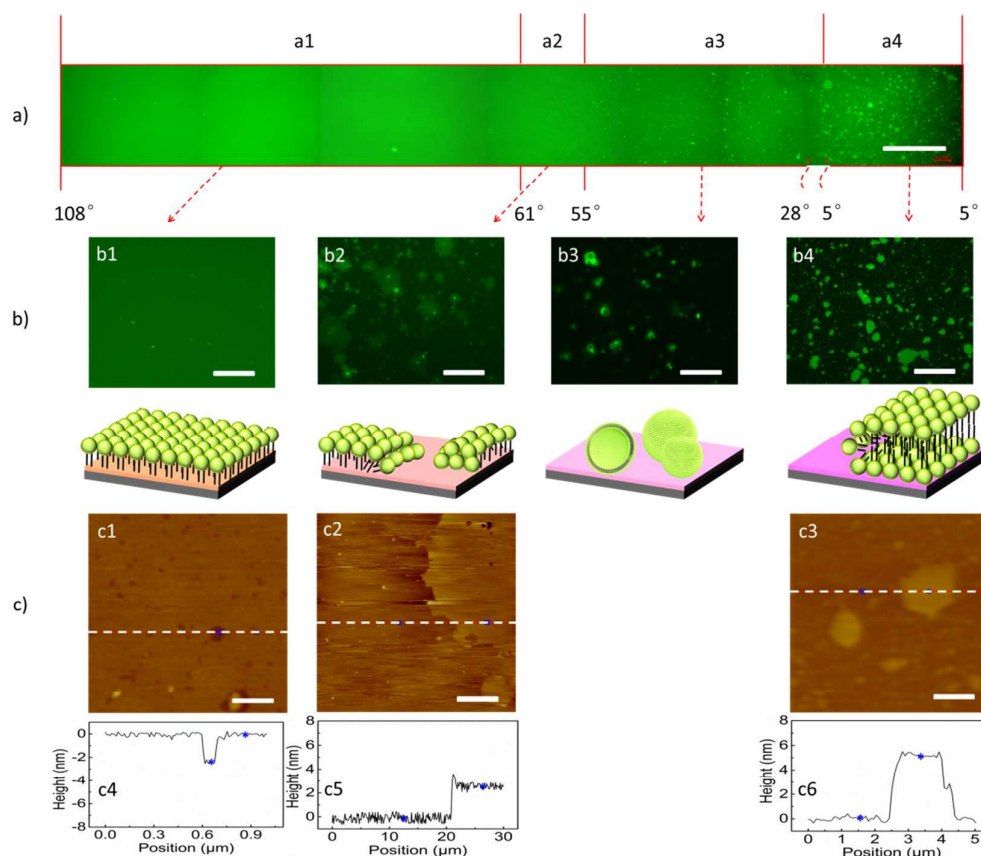


Fig. 2 Fluorescence microscopy and AFM data of lipid membranes on the contact angle gradient surface. a) The fluorescence image of the whole scene for the gradient surface after it has been incubated with the GUVs solution. The scale bar is 400 μm . b) Close-up images of different areas in a (b1-b4 corresponding to a1-a4), b1 uniform lipid monolayer, b2 lipid monolayer patches, b3 GUVs attached onto the substrate and b4 the lipid bilayer patches. The scale bar is 20 μm . At the bottom, the schematic of the supported membranes, attached GUVs and chemical surface (not to scale). c) AFM images of c1, c2, c3 are recorded in area b1, b2 and b4. Images c4-c6 are section profiles heighted along the white dash line in c1-c3. The corresponding scale bars are 200 nm, 6 μm , 1 μm , respectively.

energy and prevent homogeneous lipid monolayer formation.¹⁸

Fluorescence recovery after photobleaching (FRAP) (Fig. 3) was used to measure the diffusion coefficient D of TR-DHPE within the lipid monolayers area (Fig. 2b1). The images in Fig. 3a and 3b were taken 10 s and 10 min after photobleaching, respectively. A dark spot can be seen in the centre of the square 10 s after photobleaching, but after 10 min the fluorescence intensity is homogeneously distributed. The D

value was found to be $1.33 \pm 0.12 \mu\text{m}^2\text{s}^{-1}$ (over three samples) with a mobile fraction of 0.95, and these values are similar to those of the lipid monolayer formed on a hydrophobic surfaces ($1.0 \mu\text{m}^2\text{s}^{-1}$).¹⁹ The FRAP confirms sufficient mobility of lipids in supported monolayer.

The membrane formed with LUVs of 200 nm was also studied. On the region with contact angle below 5°, uniform bilayer is formed. The uniform bilayer is supposed to be formed by merging small bilayer patches.¹¹ The LUVs form

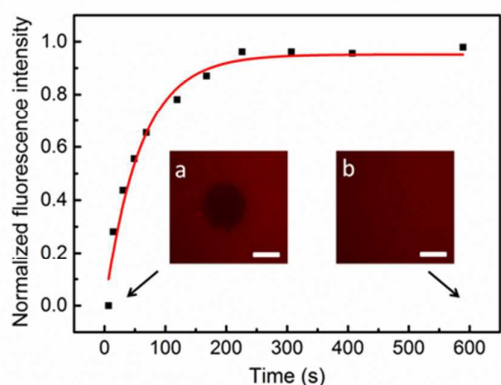


Fig. 3 The FRAP of the lipid monolayer formed on homogenous fluorescence area. Fluorescence images of the lipid monolayer were taken at a) 10 s and b) 10 min after photobleaching. Scale bar is 20 μm .

smaller patch on the surface than GUVs. Smaller patches is thermodynamically unstable than bigger ones, which leads to LUVs rupture at the edge of those patches to form continuous bilayer membrane.^{11, 20} For other areas, the membrane status is in consistent with those prepared with GUVs (Fig. S3).

In summary, we discovered that the homogenous supported lipid monolayer could be prepared using GUVs fusion method on the substrate with contact angle between $\sim 61^\circ$ and 108° . To the best of our knowledge, this is the first report of utilization of GUVs fusion in the creation of uniform supported monolayer system. The relationship between the wetting property of a surface and lipid membrane status was also revealed using a chemical gradient surface. Furthermore, the results also show that the GUVs could be intactly immobilized on the surface with contact angle from $\sim 28^\circ$ to $\sim 54^\circ$, which provides an ideal platform for transmembrane protein reconstitution.

This work was supported by the National Natural Science Foundation of China (Grant No. 21273059, 21003032, 21511130060, 21528501), State Key Laboratory of Urban Water Resource and Environment (Harbin Institute of Technology) (Grant No. 2014DX09), and Harbin Science and Technology Research Council (Grant No. 2014RFXJ063).

Notes and references

1. P. S. Cremer and S. G. Boxer, *Journal of Physical Chemistry B*, 1999, **103**, 2554-2559.
2. M. R. Cheetham, J. P. Bramble, D. G. G. McMillan, L. Krzeminski, X. Han, B. R. G. Johnson, R. J. Bushby, P. D. Olmsted, L. J. C. Jeuken, S. J. Marritt, J. N. Butt and S. D. Evans, *J Am Chem Soc*, 2011, **133**, 6521-6524.

3. Y. Zhang, L. Wang, X. J. Wang, G. D. Qi and X. J. Han, *Chem-Eur J*, 2013, **19**, 9059-9063.
4. X. J. Han, L. Wang, B. Qi, X. R. Yang and E. K. Wang, *Analytical Chemistry*, 2003, **75**, 6566-6570.
5. R. Dangla, S. C. Kayi and C. N. Baroud, *Proceedings of the National Academy of Sciences of the United States of America*, 2013, **110**, 853-858.
6. J. N. L. Albert, M. J. Baney, C. M. Stafford, J. Y. Kelly and T. H. Epps, *ACS Nano*, 2009, **3**, 3977-3986.
7. T. G. Ruardy, J. M. Schakenraad, H. C. vanderMei and H. J. Busscher, *Surface Science Reports*, 1997, **29**, 3-30.
8. K. A. Simon, E. A. Burton, Y. B. Han, J. Li, A. Huang and Y. Y. Luk, *J Am Chem Soc*, 2007, **129**, 4892-4893.
9. H. C. Yang, Q. Y. Wu, L. S. Wan and Z. K. Xu, *Chemical Communications*, 2013, **49**, 10522-10524.
10. X. J. Han, L. Wang and X. J. Wang, *Advanced Functional Materials*, 2012, **22**, 4533-4538.
11. C. Hamai, P. S. Cremer and S. M. Musser, *Biophys J*, 2007, **92**, 1988-1999.
12. G. H. Zan, C. M. Tan, M. Deserno, F. Lanni and M. Losche, *Soft Matter*, 2012, **8**, 10877-10886.
13. C. Kataoka-Hamai and T. Yamazaki, *Langmuir*, 2015, **31**, 1312-1319.
14. P. Walde, K. Cosentino, H. Engel and P. Stano, *ChemBiochem*, 2010, **11**, 848-865.
15. Y. Yu, J. A. Vroman, S. C. Bae and S. Granick, *J Am Chem Soc*, 2010, **132**, 195-201.
16. G. Staneva, M. I. Angelova and K. Koumanov, *Chemistry and Physics of Lipids*, 2004, **129**, 53-62.
17. K. Tahara, S. Tadokoro, Y. Kawashima and N. Hirashima, *Langmuir*, 2012, **28**, 7114-7118.
18. V. I. Silin, H. Wieder, J. T. Woodward, G. Valincius, A. Offenhauer and A. L. Plant, *J Am Chem Soc*, 2002, **124**, 14676-14683.
19. R. Peters and K. Beck, *Proceedings of the National Academy of Sciences*, 1983, **80**, 7183-7187.
20. I. Reviakine and A. Brisson, *Langmuir*, 2000, **16**, 1806-1815.

TOC

